IN-24
187803
p. 21

NASA Technical Memorandum 106304

Elastic-Plastic Finite Element Analyses of an Unidirectional, 9 vol % Tungsten Fiber Reinforced Copper Matrix Composite

Jose G. Sanfeliz
Lewis Research Center
Cleveland, Ohio

September 1993

(NASA-TM-106304) ELASTIC-PLASTIC FINITE ELEMENT ANALYSES OF AN UNIDIRECTIONAL, 9 VOL PERCENT TUNGSTEN FIBER REINFORCED COPPER MATRIX COMPOSITE (NASA) 21 p

N94-14719

Unclas

G3/24 0187803

NASA

ELASTIC-PLASTIC FINITE ELEMENT ANALYSES OF AN UNIDIRECTIONAL, 9 vol % TUNGSTEN FIBER REINFORCED COPPER MATRIX COMPOSITE

Jose G. Sanfeliz
National Aeronautics and Space Administration
Lewis Research Center
Cleveland, Ohio 44135

SUMMARY

Micromechanical modeling via elastic-plastic finite element analyses were performed to investigate the effects that the residual stresses and the degree of matrix work hardening (i.e., cold-worked, annealed) have upon the behavior of a 9 vol %, unidirectional W/Cu composite, undergoing tensile loading. The inclusion of the residual stress-containing state as well as the simulated matrix material conditions proved to be significant since the Cu matrix material exhibited plastic deformation, which affected the subsequent tensile response of the composite system. The stresses generated during cooldown to room temperature from the manufacturing temperature were more of a factor on the annealed-matrix composite, since they induced the softened matrix to plastically flow. This event limited the total load-carrying capacity of this matrix-dominated, ductile-ductile type material system. Plastic deformation of the hardened-matrix composite during the thermal cooldown stage was not considerable, therefore, the composite was able to sustain a higher stress before showing any appreciable matrix plasticity. The predicted room temperature, stress-strain response and deformation stages under both material conditions represented upper and lower bounds characteristic of the composite's tensile behavior. The initial deformation stage for the hardened material condition showed negligible matrix plastic deformation while for the annealed state, its initial deformation stage showed extensive matrix plasticity. Both material conditions exhibited a final deformation stage where the fiber and matrix were straining plastically. The predicted stress-strain results were compared to the experimental, room temperature, tensile stress-strain curve generated from this particular composite system. The analyses indicated that the actual thermal-mechanical state of the composite's Cu matrix, represented by the experimental data, followed the annealed material condition.

INTRODUCTION

Tungsten fiber-reinforced copper (W/Cu) is being considered for use in high-temperature, space propulsion environments, such as thrust chamber combustion liners for the space shuttle main engine (SSME). This composite system provides high thermal conductivity, creep/fatigue resistance, chemical compatibility between the fiber and matrix, and can also be fabricated by the arc-spray process, which is an appropriate technique for the production of cylindrical or conical components such as the SSME thrust chambers (refs. 1 and 2). It is of utmost importance to understand the damage behavior and deformation response of the material system before introducing it into this application. Among the specific issues that affect the behavior of metal-matrix composites (MMC's), the internal stresses generated during fabrication and the degree of work hardening of the composite matrix have to be considered in order to numerically model and study this material system with any degree of reliability.

It has been shown by several researchers (refs. 3 to 8) that the differential thermal expansion or contraction between MMC's fiber and matrix during cooldown from elevated temperatures can lead to significant plastic deformation. This is especially critical in ductile fiber/ductile matrix material systems such as W/Cu. The deformation response of another ductile matrix composite (SiC/Al) in the as-manufactured or annealed condition revealed that the matrix material hardening due to mechanical or

thermal treatments affects the overall behavior of the composite system under subsequent thermal and mechanical loads (ref. 9).

Micromechanical modeling via nonlinear finite element analyses (FEA) are performed in this study to investigate the behavior of a 9 vol %, unidirectional tungsten fiber-reinforced copper matrix composite undergoing tensile loading. Both of these analytical methodologies provide alternate and efficient means of investigating and understanding the composite behavior, by pinpointing regions where local yielding might start and propagate throughout this ductile-ductile type material. To this end, the effects of the residual stresses due to cooling from the processing consolidation temperature to room temperature are considered as well as the effects of two different matrix conditions (i.e., cold worked, annealed) on the Cu matrix. These two material conditions represent upper and lower bounds for examining the deformation of this composite system. Also, the analytical results obtained for these two cases are compared with the experimental, room temperature, tensile stress-strain curve generated from this particular copper-based composite. The main objective of this analytical approach is to provide additional qualitative information that will help in further understanding the behavior of this material system.

Composite System

The W/Cu composite system being studied is manufactured in the form of four-ply panels using an arc-spray technique (ref. 1). The matrix is oxygen-free, high-conductivity (OFHC) copper (99.95 wt % Cu) and the fibers are General Electric 218CS continuous tungsten wire of 200-μm (8-mil) diameter. The composite plates contained unidirectional tungsten fibers arranged in a square packing array, with a fiber volume percent of 9 (ref. 10). Based on this material description, the assumptions used for the finite element model and nonlinear finite element analyses are presented and discussed in the following sections.

APPROACH

Finite Element Modeling

A three-dimensional, finite element, square packing representative unit cell of the $[0°]_4$, 9 vol % composite was generated with the aid of COMGEN (ref. 11). COMGEN (COmposite Model GENerator) is an in-house computer code developed by the Structural Mechanics Branch at NASA Lewis Research Center, which creates geometric and discrete composite models in a PATRAN (ref. 12) data base. PATRAN is the finite element pre- and post-processor used in this study. The finite element model (fig. 1) consisted of 1449 nodes, 1024 eight-noded, solid, isoperimetric elements. The volume for this representative unit cell of same width, thickness, and depth is $(5.91\ d)^3$, where d is the diameter of the tungsten wire. This micromechanical model represents a cross section of the composite material subjected to mechanical loading. The use of this type of elements for inelastic analysis has proven to give adequate results where incompressible or nearly incompressible behavior occurs (refs. 12 and 13), therefore, they will be utilized for the analysis portion of this effort. Note that the shaded regions in the model depicted by figure 1 represent the composite fibers.

Nonlinear Finite Element Analyses

Elastic-plastic finite element analyses were performed numerically with the nonlinear finite element program MARC (ref. 13). The three-dimensional brick elements mentioned beforehand correspond to element number 7 of the MARC library. The numerical procedure is based upon the von Mises yield

criterion, the Prandtl-Reuss flow rule, and the isotropic hardening theory. Since the effects of the residual stresses during manufacture play an important role on the subsequent composite behavior, the analyses considered the stresses due to one cooldown cycle, from an assumed stress-free, upper-limit temperature equal to 542 °C (1008 °F) down to room temperature (RT) 26 °C (79 °F). This upper limit temperature (below the consolidation temperature) corresponds to half the absolute melting temperature (T_m) of the Cu matrix (1084 °C = 1983 °F). This assumption has been adopted by several researchers (refs. 4, 5, and 9) in order to avoid the significant viscoplastic (i.e., rate dependent) material behavior present at temperatures above half the matrix material T_m.

Temperature dependent constituent material properties such as yield stress (σ_y), Young's modulus (E), and thermal expansion coefficient (α) were included for both the W fiber and Cu matrix, to insure that the history of plastic deformation during cooling from the stress-free temperature to ambient was accurate. Tables I and II summarize the temperature dependent properties used in the analyses for the 218CS W fiber and the OFHC Cu matrix (refs. 14 to 17), respectively. Note that the degree of work hardening for the copper matrix (cold-worked, annealed) is considered by assigning the corresponding temperature-dependent, yield stress values to the matrix elements. Also, the annealed yield stress values correspond to expected minimums for this material condition (ref. 16). The amount of hardening or softening used to determine how much plastic strain the Cu matrix experienced after it yielded at several given temperatures was assumed to be the same as the RT work hardening values. This is a reasonable approximation since available experimental stress-strain curves at high temperatures exhibited the same hardening/softening slopes in their corresponding inelastic regions (refs. 16 and 18).

The effects of plasticity (or yielding) were represented by including the experimental stress-strain, RT curves for the ductile W fiber (ref. 15) and ductile Cu matrix (refs. 16 and 18). Both curves were entered as piecewise linear representations in which multiple work hardening slopes were considered to deal with the inelastic (plastic) material behavior. Again, the material conditions were included through these stress-strain curves as depicted in figure 2. The stress-strain curve for the fully annealed Cu was approximated from the experimental, expected minimum yield stress at RT and the work hardening slopes calculated from the available high temperature, experimental stress-strain curves for this specific material condition. Note that this assumption was needed to maintain the compatibility between the hardening condition values and the temperature-dependent data, since uniform experimental properties for the annealed Cu were quite difficult to obtain. The hardened Cu stress-strain curve exhibits a considerably higher yield strength at RT than the fully annealed Cu curve (417 MPa or 60.5 ksi versus 35 MPa or 5.08 ksi) and there is even some small strain-softening behavior, as opposed to the positive work hardening slopes of the annealed condition.

Constraints on the model were intended to provide a generalized plane strain condition. The basic assumptions for this boundary condition state that (1) the nodes on the free faces of the unit cell (boundary planes) should remain planar with one another if any displacements take place and (2) that the shearing deformations in the structure are negligible (refs. 3, 9, and 12). This behavior is characteristic of a typical cross section through a continuous, infinitely long composite, such as the composite model depicted in figure 1. The nodes along the top X-Z face, the right side Y-Z face, and the back X-Y face have zero displacements in their normal directions to simulate the effect of the rest of the material, while the nodes along the bottom X-Z face, the left side Y-Z face and the front X-Y face are coupled in their normal directions through the use of multipoint or tying constraints.

One very important aspect of this composite system is the strong bond that exists between the W fiber and the Cu matrix. This assumption applies only to the initial portions of the composite stress-strain curve being studied, since near failure fiber/matrix debonding can be an issue (ref. 22). Reference 12 demonstrated the case in which fiber/matrix debonding of a SiC/Ti-15-3 material system under

tensile loading did occurred, therefore, this event was accounted in the nonlinear FEA by incorporating gap elements between the fiber and matrix elements to model the interface region.

The mechanical loads imposed on the model were uniform pressure loads applied perpendicular to the front X-Y face as shown in figure 1. Very small loading increments were used until the strain level at which the W fibers have been experimentally observed to fracture. The selection of the load increment to solve the nonlinear analysis involved several approaches. One extreme is to use a large number of small steps with few iterations. The other extreme is to solve one large step with many iterative cycles. The optimum approach is to employ a combination of both, such that equilibrium is satisfied at the end of each load step (ref. 13). All of these approaches were investigated for each matrix hardening condition and the obtained numerical results for each case did not differed considerably. This loading condition simulated the uniaxial tensile behavior in the material. The composite strains were calculated from the displacements of the entire model and not of individual elements (ref. 12). Because the applied stress field on the representative unit cell is uniform (constant), the composite stress becomes equal to the applied stress (ref. 19). From these numerical values, the global response of the composite can be characterized and the material's experimental stress-strain response can be directly compared with the analyses. The previously-defined modeling and analysis assumptions were applied to study this composite system. The nonlinear FEA and their corresponding results are outlined and discussed in the following sections.

Matrix Hardening Conditions.—Two different hardening levels of the composite matrix material were considered as follows: (1) an unidirectional W fiber-reinforced OFHC Cu under a cold-worked condition and (2) an unidirectional W fiber-reinforced OFHC Cu under an annealed condition. Both analysis models are subjected to a thermal cooldown of $\Delta T = -516$ °C (-961 °F), followed by a tensile mechanical load. Perfect bonding between the W fiber and Cu matrix with no fiber/matrix debonding is assumed. The results will focus upon the effects that residual stresses have on the material behavior and subsequently upon the deformation stages developed under the application of mechanical load.

RESULTS

Deformation During Thermal Cooldown Stage

Predicted Plastic Deformation.—The first set of results consist of the predicted plastic deformation of the W/Cu composite from cooldown. Because of the appreciable difference between the W fiber and Cu matrix coefficients of thermal expansion ($\alpha_{Cu} \approx 4\ \alpha_W$), the temperature change as the composite is cooled to RT can induce the matrix to yield plastically (refs. 3, 7, and 8). The formation of the plastic zone in the annealed matrix material begins almost immediately in the matrix elements surrounding the fibers, and spreading evenly towards the remaining outside matrix elements. This trend can be seen in figures 3 to 6 which illustrate the regions of plastic deformation at various stages of cooling. The regions in which plastic deformation occurs at various temperatures are shaded.

On the other hand, the W/Cu composite containing the cold-worked matrix does not exhibit any considerable plastic yielding of the Cu matrix elements, throughout the cooldown stage to RT. There is, however, some indication of plastic deformation at the center of two W fibers located along the top X-Z face of the composite model (fig. 6(a)). These two specific fibers began exhibiting a small plastic zone at temperatures between 181 °C (358 °F) and 129 °C (264 °F). At these temperature values, tungsten still exhibits a ductile behavior (ref. 17) and it is possible for this material to yield. Also, the artificial effects induced by the generalized plane strain boundary conditions upon the representative unit cell, may have some influence on these corner and top face fibers' behavior.

Residual Stresses.—The predicted Cu matrix and W fiber longitudinal residual stresses at RT for both material conditions exhibit the expected behavior (figs. 7 and 8, respectively). Tensile stresses on the Cu matrix are developed since the matrix contracts much faster than the fibers during cooldown and therefore, in order to maintain continuity with the fibers, the matrix elements must stretch axially, creating this tensile stress state (refs. 3, 7, and 8). A compressive longitudinal residual stress must then exist on the W fibers for each corresponding material condition. The Cu matrix longitudinal residual stress values for the annealed material condition are much lower than the values obtained from the hardened material condition, and therefore, their influence upon the corresponding W fibers will not be as severe as for the cold-worked state. Figure 7 depicts the matrix regions in which the longitudinal residual stress values are more significant. The presence of these residual stresses and of the previous plastic deformation will prove to be significant factors in defining the subsequent tensile behavior of this composite system.

Overall residual stresses were characterized by calculating the equivalent (effective) von Mises stress. Note that for the von Mises yield criterion, yielding occurs when the effective stress reaches the uniaxial yield strength (σ_y) of the material (ref. 4). Examining the matrix thermal residual stresses at RT for the cold-worked material condition, the Cu matrix regions adjacent to the W fibers indicate the location of probable plastic yielding (Fig. 9(a)). This zone is strictly localized and includes only a small region between the composite's fiber/matrix boundary, while excluding the rest of the matrix elements, which are stressed below their material yield strength. The overall behavior upon the material system was clearly demonstrated in figure 6(a), in which the plastic deformation of the composite for the cold-worked condition is negligible. Recall that for this hardened material condition, the Cu matrix yield strength is 417 MPa (60.52 ksi) (ref. 17).

The equivalent Mises stress values on the Cu matrix at RT, for the annealed material condition (fig. 9(b)) ranged from 39.30 MPa (5.7 ksi) up to 42 MPa (6.09 ksi). In this case, the Cu matrix yield strength is equal to 35 MPa (5.08 ksi) (ref. 16). For this annealed-matrix material all of the matrix elements have yielded, however, only the matrix near the fiber/matrix interface yielded in the case of the cold-worked matrix. Due to the high plastic flow of the annealed Cu matrix, the residual stresses are not as high as obtained from a cold-worked condition.

The equivalent Mises stress values for the fibers under cold-worked and annealed material conditions remained constant. The fiber's equivalent stress values for the cold-worked material condition were equal to 1342 MPa (194.78 ksi) while for the annealed material condition these values were equal to 412 MPa (59.80 ksi). Since the matrix is flowing plastically, the residual stresses on the W fibers are reduced. Therefore, the W fibers under the annealed material condition do not exhibit any plastic yielding as opposed to the cold-worked material state, in which the fibers show some local yielding, attaining equivalent Mises stress values greater than the W material yield strength of 1304 MPa (189.26 ksi) (ref. 15). This behavior might explain why there is some plastic deformation present at RT on some W fibers under this hardened material condition.

Deformation During Tensile Mechanical Loading

Deformation Stages.—The predicted RT, tensile stress-strain response for the 9 vol % W/Cu composite model is shown for both the cold-worked and annealed material conditions in figure 10. Also shown in figure 10 is a portion of the experimentally obtained stress-strain curve (ref. 22), up to the strain level at which the W fibers began to fail. This behavior has been previously observed on W/Cu composites with low volume fraction values (ref. 20), such as the one being studied. When compared to the experimental data, it is obvious that these material conditions represent upper and lower bounds

which depict the characteristic deformation stages present on this MMC system. The starting condition for these predictions is the residual stress-containing state, which was described in the previous section.

Beginning with the cold-worked material condition, the predicted stress-strain RT curve exhibits three deformation stages. Stage I is denoted by a region of high slope (region AB), stage II by a region of reduced slope (region BC), and finally stage III (region CD), a region of almost zero slope having the characteristic of a perfectly plastic solid. The matrix is the major load-carrying component for this composite system of low fiber content. The Cu matrix did not show any previous, considerable plastic flow due to thermal cooldown, therefore, it is possible for the composite to exhibit this matrix dominated, elastic behavior under stage I. Stage II corresponds to the case in which the fibers continue to strain elastically, while the matrix begins to exhibit considerable plastic deformation. Stage III represents a state where both the fiber and matrix are straining plastically. This behavior will continue until the ultimate strength of the fibers is reached and they start to fail. These characteristic stages of deformation were observed by previous researchers (ref. 21) while investigating and analyzing the behavior of these metal-matrix composite systems, and the numerical results obtained for this material condition simply represent one possible explanation of the deformation mechanisms.

The predicted RT deformation stages present in the composite with an annealed matrix correspond to a stage II and stage III behavior, as indicated by regions B′C′ and C′D′ in figure 10, respectively. The matrix behavior of this composite system is again the dominating factor since the induced plasticity of the Cu matrix during cooldown significantly affected the tensile behavior. The predicted presence of this high plastic deformation on the matrix implies that tensile deformation should proceed at a lower stress level than for the previous cold-worked state. Thus, for the annealed-matrix composite, the onset of stage II becomes so low that stage I (elastic matrix deformation) behavior does not appear on the composite response. Based on the significant effect that the previous plastic deformation has upon the overall tensile response of the composite, the propagation of the plastic zones/regions among both material conditions will be examined for each particular deformation stage. Again, these results serve as guidelines for confirming the expected trends.

Propagation of Plastic Zone.—Stage I (region AB) type behavior was only present under the cold-worked state as previously shown in figure 10. The region where there is some appreciable plastic flow under this deformation stage corresponds to the fiber/matrix boundary. This localized plastic zone begins to propagate towards the adjacent matrix elements surrounding the W fibers, as the mechanical load is increased. It was indicated in the thermal cooldown section that the elements contained in this small area were stressed above the matrix yield strength, therefore, the application of mechanical loads would initiate the propagation of considerable plasticity on these highly stressed regions. Figure 11(a) shows these small regions of predicted plastic deformation at an applied tensile stress of 145 MPa (21.04 ksi). Even though the only other region exhibiting some previous plasticity corresponds to the two W fibers located along the top X-Z face of the model, the numerical difference between equivalent Mises stress values for the W fibers under this hardened matrix condition was negligible. The rest of the matrix elements do not exhibit any plastic yielding. Even after increasing the tensile load to 175 MPa (25.4 ksi) and to 280 MPa (40.64 ksi), the plastic zone remains localized around the W fiber/Cu matrix boundary. Figures 12(a) and 13 depict these shaded regions, respectively.

Stage II (region BC) behavior for the cold-worked material condition is further demonstrated in figure 14, where the predicted areas of matrix plasticity propagate extensively throughout the composite system. The W fibers still remain elastic at this applied stress level of 380 MPa (55.15 ksi), even though they have started to sustain more of the load previously carried by the matrix. Examining the annealed material condition under this same deformation stage (fig. 17), which is denoted by region B′C′, the extent and amount of matrix plasticity is more extensive at an applied representative load of 70 MPa

(10.16 ksi) due to high plastic deformation generated during the cooling process to RT (fig. 6(b)). As the applied stress is increased to 145 MPa (21.04 ksi) the regions of greater matrix plasticity coincide with sections of the composite that were subjected to high tensile residual stresses at RT (fig. 7(b)). Also, the fiber/matrix boundary areas for this annealed state exhibit a higher plastic deformation than the cold-worked material under the same applied load of 145 MPa (21.04 ksi), as clearly shown in figure 11(b). These local areas also showed the highest equivalent Mises stress values at RT.

The beginning of stage III (region CD) behavior under a cold-worked state is indicated by the increase on Cu matrix plastic flow, for an applied load of 480 MPa (69.67 ksi) (fig. 15). Even the W fibers exhibit some evidence of plasticity since they are assuming the role of major load-carrying components at this stage. Regions of large plastic strain begin to form on the matrix elements around and along the W fibers, and as the applied load was increased up to 500 MPa (72.57 ksi), these regions exhibited the largest concentration of plastic flow at the end of the current deformation stage (fig. 16). The W fibers exhibit appreciable plastic flow due to the inability of the matrix material to sustain any further load. The center of the two W fibers that exhibited some previous plasticity because of the thermal cool-down, also showed a concentrated amount of plasticity under this loading stage. However, these regions did not propagate from the core of the fiber towards its outside sections and remained quite localized.

The annealed material condition also exhibits full plastic deformation for the matrix as well as the fibers under this deformation stage (region C'D'). At an applied stress of 160 MPa (23.23 ksi), the same matrix regions that exhibited the highest plastic flow under stage III, cold-worked conditions, also showed the highest concentrations of plastic yielding on the composite (fig. 18). The amount of plastic deformation was much greater in this annealed state because the plastically-deformed matrix state after cooldown was more severe for this composite than for the hardened material condition. Further increasing the load to 175 MPa (25.4 ksi) the plastic zone of highest value has spread through all of the matrix, causing the fibers to take all of the load thus, increasing their plastic deformation (fig. 12(b)). Both final load values representing the end of stage III deformation under cold-worked and annealed material conditions (500 and 175 MPa, respectively), correspond to the stress under which the experimental strain level of the composite is reached, before the W fibers began failing. However, for the annealed condition, this load is only 35 percent of the stress necessary to cause this final deformation stage under a cold-worked material state.

DISCUSSION

The results described in the previous section demonstrate the significance of the residual stresses upon the subsequent tensile mechanical behavior of the composite system. This effect was also enhanced by the material work hardening conditions that were considered for this ductile fiber/ductile matrix type system. The total amount of predicted plastic deformation and its distribution throughout the composite for the cooldown cycle, were important factors in this study. Because the Cu matrix undergoes extensive plastic deformation under the presence of residual stresses, the annealed composite system will start yielding immediately upon loading. On the other hand, the finite element method predicted that the Cu matrix under a hardened material condition would not be deformed as severely by the thermal cooldown stage and therefore, the subsequent composite deformation will exhibit a different tensile behavior. Even though the tensile residual stresses present on the matrix regions for both material conditions were of different magnitude, the sections that exhibited large stress gradients were more prone to deform plastically during the application of a tensile mechanical load. That region exhibiting high plastic flow will yield at a lower value of applied stress than a material system without residual stresses. The matrix residual stresses did influence the fiber behavior under this cooling cycle. This was the case for the cold-worked material condition in which the exerted residual stresses on the W fibers were large enough to

initiate some plastic deformation at higher temperatures. The plastically deformed fiber regions were not widespread and eventually, their impact upon the overall composite behavior was only significant at the end of the loading stage (stage III).

The propagation of the plastic zone under tensile loading, for both material conditions, began around the fiber/matrix boundary, spreading towards the adjacent and outside Cu matrix elements. The only difference being that these regions were predicted to be very localized for the cold-worked state while for the annealed condition the plastic zone was quite widespread throughout the rest of the matrix elements as well. This trend agrees with the observed behavior on other ductile metal matrix systems such as aluminum (ref. 3) in which the deformation in tension involves initial plasticity in the regions between the cylindrical surfaces where the fiber and matrix meet.

The predicted stress-strain response based on these material conditions represented characteristic upper and lower bounds of the composite behavior. Even though the predicted stress-strain response did not match exactly the experimentally observed behavior, the method provided additional insight towards explaining this material's actual mechanical response. The analysis indicates that the actual thermal-mechanical state of the matrix in the composite represented by the experimental data falls somewhere between annealed and cold-worked. This should not be surprising given the processing cycle used for manufacture of the composite. Whenever analyses are performed to predict composite deformation behavior after joining operations such as welding and diffusion bonding, one must account for these sort of effects since they can greatly affect the overall composite mechanical behavior (ref. 22).

There were three distinctive deformation stages present under the cold-worked material condition. The first stage (stage I) denoted a region of high slope where the existence of some plastic deformation was concentrated solely around the fiber/matrix boundary, up to the limiting load of this stage (280 MPa or 40.64 ksi). This stage was not predicted under the annealed material condition since the Cu matrix exhibited a very high plastic flow after cooldown, which affected this composite response in a significant manner. The second deformation stage (stage II) consisted of a region of reduced slope which demonstrated a considerable plastic deformation of the matrix material and finally, a third stage (stage III) where the W fibers exhibited appreciable plastic flow due to the inability of the matrix to carry any further load. This stage was also predicted for the annealed material condition, but because of the severe effects of the previous plastically-deformed state, the composite yielded at lower applied stress values. These deformation stages demonstrated the matrix dominated behavior for this composite system since the Cu matrix plastic deformation reduced its load-carrying capabilities and hence, shifted all the load distribution towards the W fibers, causing them to eventually flow plastically.

A very important requirement for the Cu matrix of these perfectly bonded MMC's is to exhibit sufficient ductility, such that the material would withstand thermal shock and impact loads. Since the W fibers showed some plastic flow, the matrix must undergo sufficient strain to allow the fiber to reach its ultimate strength (ref. 21). This composite behavior was predicted through both work-hardening conditions but, it was clearly shown by the annealed material state which followed the experimental stress-strain trends. The analytical approach considered the inelastic behavior of both constituent components. This material behavior simulation proved to be quite significant on the overall analysis process since the compatibility of the hardening curves data with the yield strength temperature dependency affects the composite response. That is, great care must be exercised when selecting the yield strength, temperature-dependent values that correspond exactly to the same experimental stress-strain material curves, especially for a matrix material such as Cu, which is highly dependent on prior thermal-mechanical processing. Different Cu matrix yield strength values would change the point at which plastic yielding would begin, thus affecting the overall response of this matrix dominated composite. Also, time dependent (creep) deformation

or recovery of the matrix may be important under these types of analyses for other composites, and therefore should be considered in the general case.

SUMMARY

A micromechanical model via nonlinear finite element analyses were performed to investigate the behavior of a 9 vol %, unidirectional tungsten fiber-reinforced copper matrix composite undergoing tensile loading. The model represented a typical cross section through the continuous composite material. The elastic-plastic analyses considered the residual stresses during cooldown as well as the effects of two different matrix work hardening conditions. The main objectives of this analytical approach were to provide additional qualitative information and a complementary means of understanding the behavior of this ductile-ductile type material system.

The results indicated that the amount of plastic deformation developed during the thermal cooldown of the composite had a dominant effect upon the subsequent tensile behavior. The corresponding work hardening conditions also influenced the material's behavior as demonstrated by the predicted tensile load deformation stages and the propagation of their corresponding plastic zones. The cold worked matrix composite exhibited an initial stage (stage I) where the Cu matrix was not deformed considerably, therefore, the composite was able to handle a higher load range as compared to the annealed state which exhibited an initial deformation stage showing extensive matrix plasticity (stage II). This stage was followed by both the W fiber and Cu matrix undergoing plastic deformation (stage III). The extensive matrix plasticity prompted this matrix dominated composite to transfer its load-carrying capacity to the ductile fibers, eventually causing them to yield. This deformation stage was also present under a hardened material condition but, it occurred at an expected higher stress range. The analytical stress-strain curves were compared with the experimental, RT, stress-strain response of the composite and demonstrated that the actual Cu matrix followed a fully annealed material condition. The predicted composite stress-strain response provided initial limiting values towards the prediction of this composite's behavior. Future studies could involve using this modeling approach to further confirm this composite system's observed deformation mechanisms, thus providing additional insight towards understanding their constitutive response and failure conditions. Micromechanical modeling in conjunction with finite element analysis are not only versatile tools essential for understanding the mechanical behavior of composites, but also serve as companions to selective experiments for overall reduced time/cost of material evaluation, material development and component design.

ACKNOWLEDGMENTS

The author would like to thank Michael J. Verrilli and Louis J. Ghosn for the experimental, W/Cu stress-strain data and for many helpful discussions, Matthew E. Melis for his assistance and comments on the FE modeling, Hee Mann Yun and David L. Ellis for providing the W and OFHC Cu experimental properties and Alan D. Freed for providing additional constituent material properties and very useful feedback.

REFERENCES

1. Westfall, L.J.; and Petrasek, D.W.: "Fabrication and Preliminary Evaluation of Tungsten Fiber Reinforced Copper Composite Combustion Chamber Liners," NASA TM-100845, 1988.

2. Doychak, J.: "Metal- and Intermetallic-Matrix Composites for Aerospace Propulsion and Power Systems," JOM, Vol. 44, No. 6, June 1992, pp. 46–51.

3. Levy, A.; and Papazian, J.M.: "Elastoplastic Finite Element Analysis of Short-Fiber-Reinforced SiC/Al Composites—Effects of Thermal Treatment," Acta Metallurgica et Materialia, Vol. 39, Oct. 1991, pp. 2255–2266.

4. Arnold, S.M.; and Wilt, T.E.: "Influence of Engineered Interfaces on Residual Stresses and Mechanical Response in Metal Matrix Composites," NASA TM–105438, 1992.

5. Ghosn, L.J.; and Lerch, B.A.: "Optimum Interface Properties for Metal Matrix Composites," NASA TM–102295, 1989.

6. Pindera, M.-J.; Freed, A.D.; and Arnold, S.M.: "Effects of Fiber and Interfacial Layer Architectures on the Thermoplastic Response of Metal Matrix Composites," NASA TM–105802, 1992.

7. Daehn, G.S.; Anderson, P.M.; and Zhang, H.: "Temperature Change Induced Plasticity in Metal Matrix Composites—Effects of Reinforcement Morphology," Scripta Metallurgica et Materialia, Vol. 25, Oct. 1991, pp. 2279–2284.

8. Larsson, L.O.K.: "Thermal Stresses in Metal Matrix Composites," in International Conference on Composite Materials II, Apr. 1978, pp. 805–821.

9. Li, D.S.; and Wisnom, M.R.: "Nonlinear Stress-Strain Behavior of Unidirectional Silicon Carbide Fibre Reinforced Aluminium Alloy," Journal of Strain Analysis for Engineering Design, Vol. 27, No. 3, July 1992, pp. 137–144.

10. Verrilli, M.J.; Kim, Y.-S.; and Gabb, T.P.: "High Temperature Fatigue Behavior of Tungsten Copper Composites," NASA TM–102404, 1989.

11. Melis, M.E.: "COMGEN—A Computer Program for Generating Finite Element Models of Composite Materials at the Micro Level," NASA TM–102556, 1990.

12. Lerch, B.A.; Melis, M.E.; and Tong, M.: "Experimental and Analytical Analysis of Stress-Strain Behavior in a $[90°/0°]_{2s}$, SiC/Ti-15-3 Laminate," NASA TM–104470, 1991.

13. MARC General Purpose Finite Element Program (Rev. K.4, Jan. 1990), MARC Analysis Research Corporation, Palo Alto, CA.

14. Freed, A.D.; and Walker, K.P.: "Refinements in a Viscoplastic Model," NASA TM–102338, 1989.

15. Yun, H,M.: Private Communication, Materials Division, Advanced Metallics Branch, NASA Lewis Research Center, Cleveland, OH, 1992.

16. Rockwell International, Rocketdyne Division, Materials Properties Manual, Fourth Edition, First Printing, 1987.

17. American Society for Metals, Properties and Selection: Nonferrous Alloys and Special-Purpose Materials/Metals Handbook, Tenth Edition, Vol. 2, ASM International, 1990.

18. Freed, A.D.: Private Communication, Materials Division, NASA Lewis Research Center, Cleveland, OH, 1992.

19. Tsai, S.W.; and Hahn, H.T.: Introduction to Composite Materials. Lancaster, PA: Technomic Publishing Company, Inc; 1980.

20. Ozawa, E.; and Watanabe, O.: "The Role of the Workhardening in the Mechanical Behavior of Metal Fiber-Metal Composites," in Proc. Japan-U.S. Conference, Tokyo, 1981, pp. 204–212.

21. McDanels, D.L.: "Tungsten Fiber Reinforced Copper Matrix Composites," NASA TP–2924, 1989.

22. Verrilli, M.J.: Private Communication, Structures Division, Fatigue and Fracture Branch, NASA Lewis Research Center, Cleveland, OH, 1993.

TABLE I.—218CS TUNGSTEN (W) TEMPERATURE-DEPENDENT MATERIAL PROPERTIES USED IN THE FINITE ELEMENT ANALYSES

[Poisson's ratio = 0.28][a]

Temperature, °C	Thermal expansion coefficient[a], α, 1/°C	Young's modulus[a], E, GPa	Yield Stress[b], σ_y, MPa
26	4.404×10^{-6}	394.922	1303.57
82	4.413	394.630	1241.07
138	4.422	394.168	1178.57
195	4.431	393.525	1107.14
251	4.440	392.722	1053.57
307	4.449	391.749	1000.00
364	4.458	390.585	946.43
420	4.467	389.271	892.86
476	4.476	387.788	842.86
533	4.485	386.104	776.79
702	4.512	380.080	687.50
871	4.539	372.513	580.36

[a]Reference 14.
[b]Reference 15.

TABLE II.—OFHC COPPER (CU) TEMPERATURE-DEPENDENT MATERIAL PROPERTIES USED IN THE FINITE ELEMENT ANALYSES

[Poisson's ratio = 0.34][a]

Temperature, °C	Thermal expansion coefficient[a], α, 1/°C	Young's modulus[a], E, GPa	Yield Stress, σ_y, MPa	
			Cold-Worked[d]	Annealed[c]
26	16.13×10^{-6}	125.916	417	35
82	16.41	123.457	390	35
138	16.69	120.828	360	35
195	16.98	117.978	330	30
251	17.26	115.008	285	28
307	17.54	111.868	240	25
364	17.82	108.499	180	22
420	18.10	105.017	85	20
476	18.38	101.366	40	18
533	18.67	97.477	20	17
702	19.51	84.912	0	10
871	20.36	70.806	0	5

[a]Reference 14.
[c]Reference 16.
[d]Reference 17.

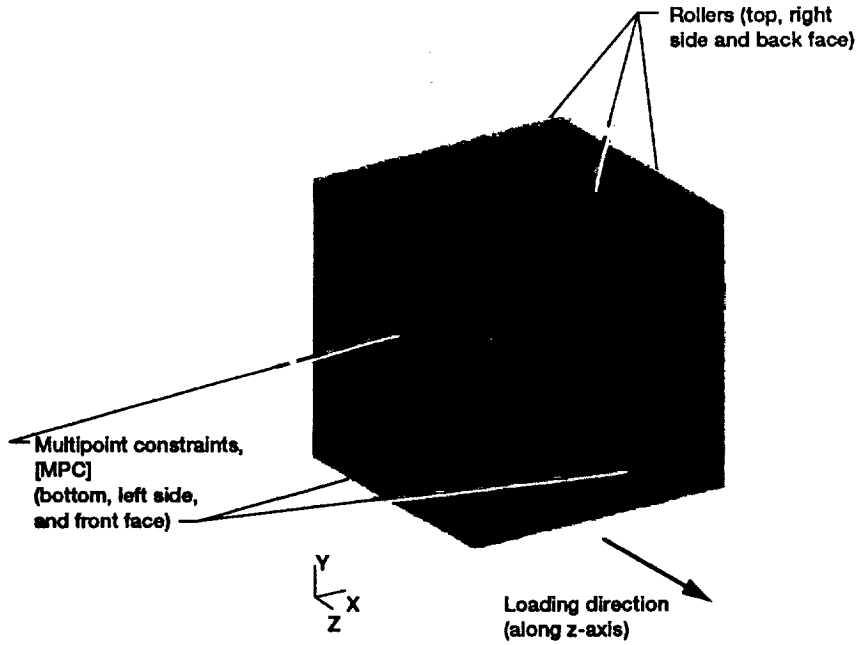

Figure 1.—Micromechancal FE model of the tungsten fiber-reinforced copper matrix, unidirectional composite.

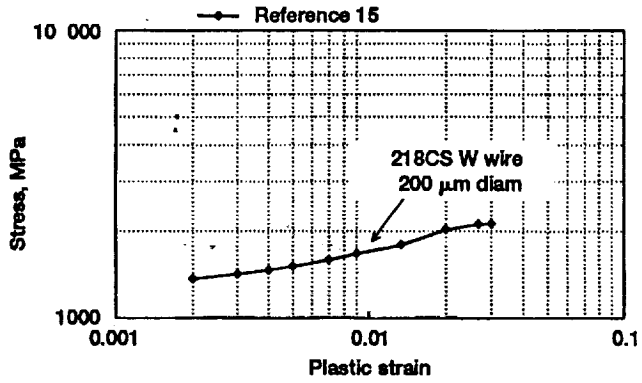

(a) Stress-plastic strain for GE218CS W wire.

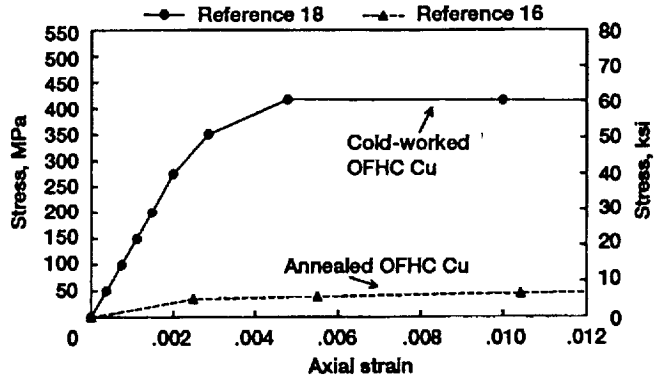

(b) Stress-axial strain for cold-worked and annealed OFHC Copper.

Figure 2.—Experimental stress-strain curves at room temperature.

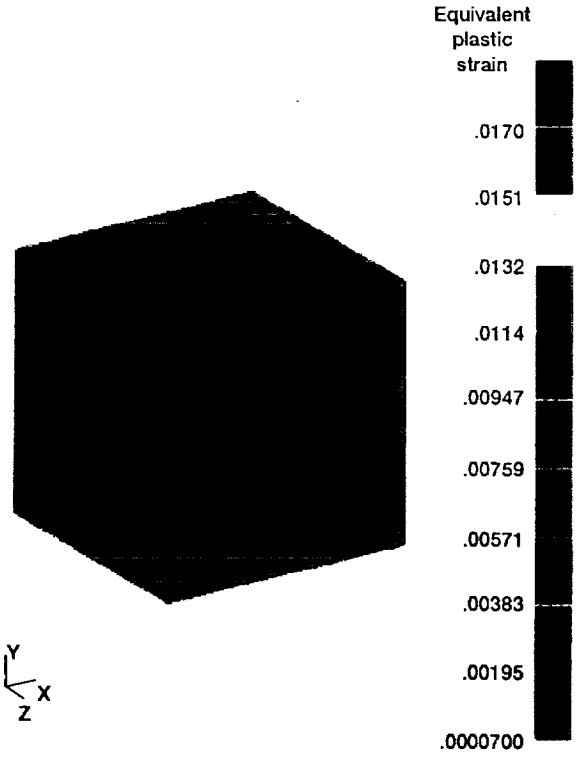

Figure 3.—Predicted plastic deformation at 284 °C, after cooldown from 542 °C of a 9 v/o W/Cu composite under annealed material conditons.

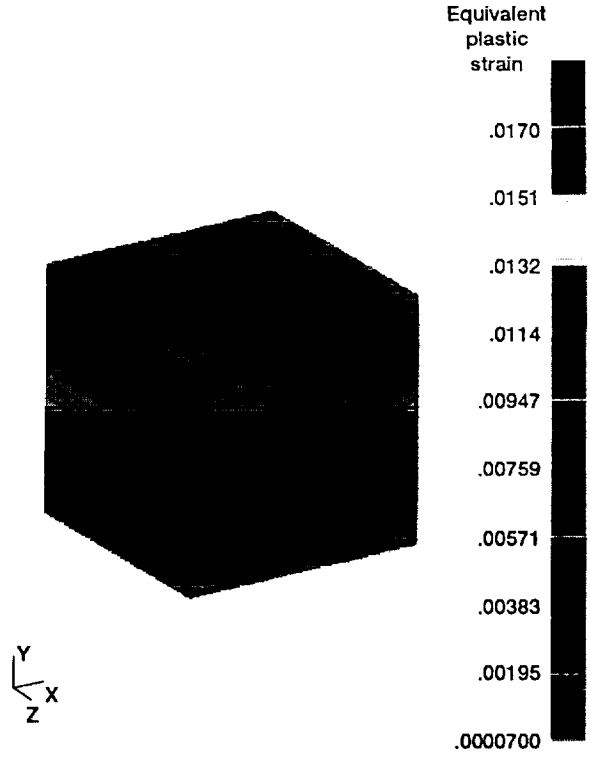

Figure 4.—Predicted plastic deformation at 129 °C, after cooldown from 542 °C of a 9 v/o W/Cu composite under annealed material conditons.

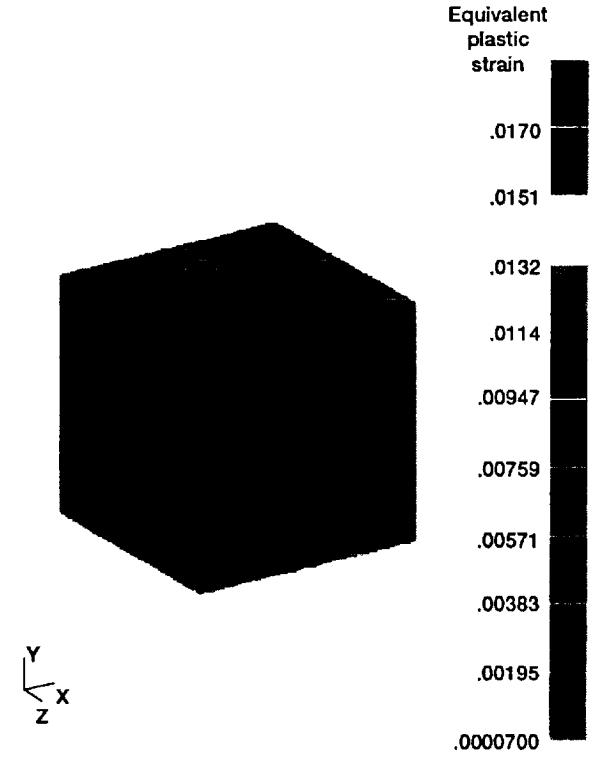

Figure 5.—Predicted plastic deformation at 78 °C, after cooldown from 542 °C of a 9 v/o W/Cu composite under annealed material conditions.

PRECEDING PAGE BLANK NOT FILMED

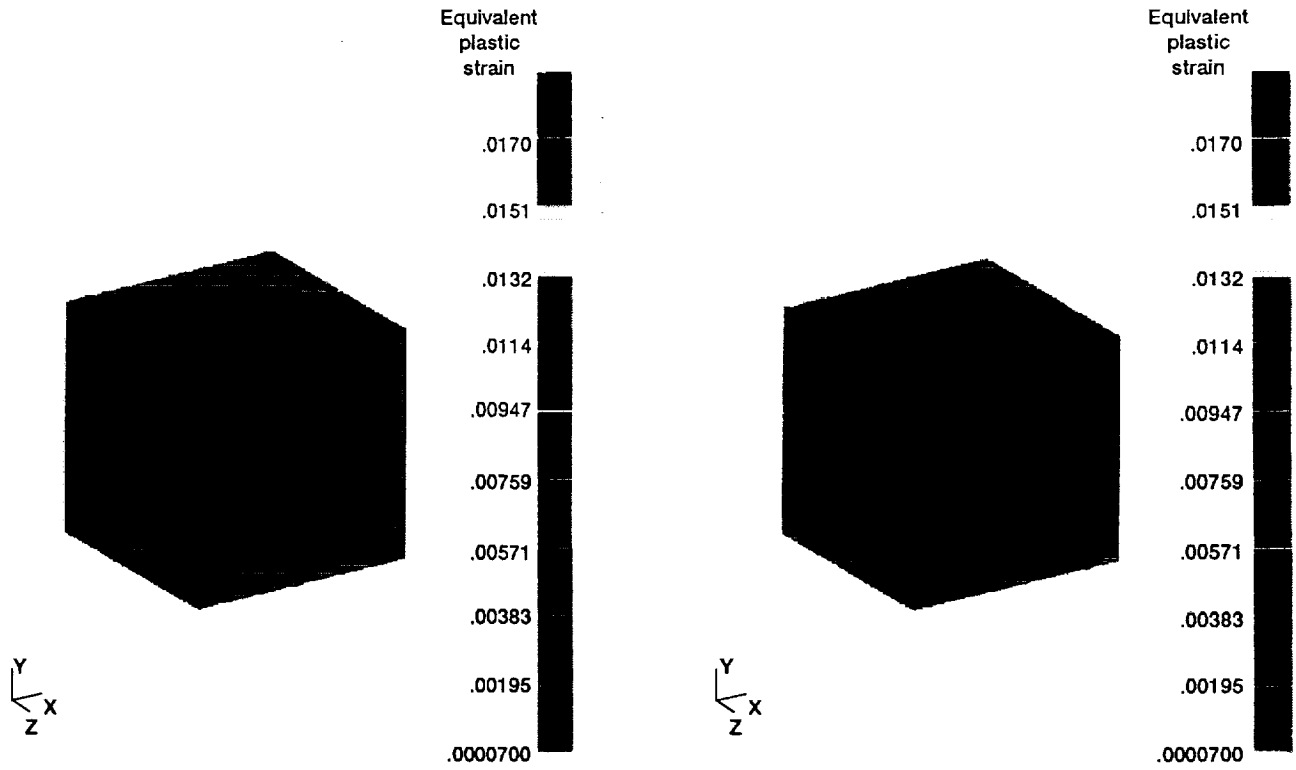

(a) Under cold-worked conditions.

(b) Under annealed material conditions.

Figure 6.—Predicted plastic deformation at RT, after cooldown from 542 °C of a 9 v/o W/Cu composite.

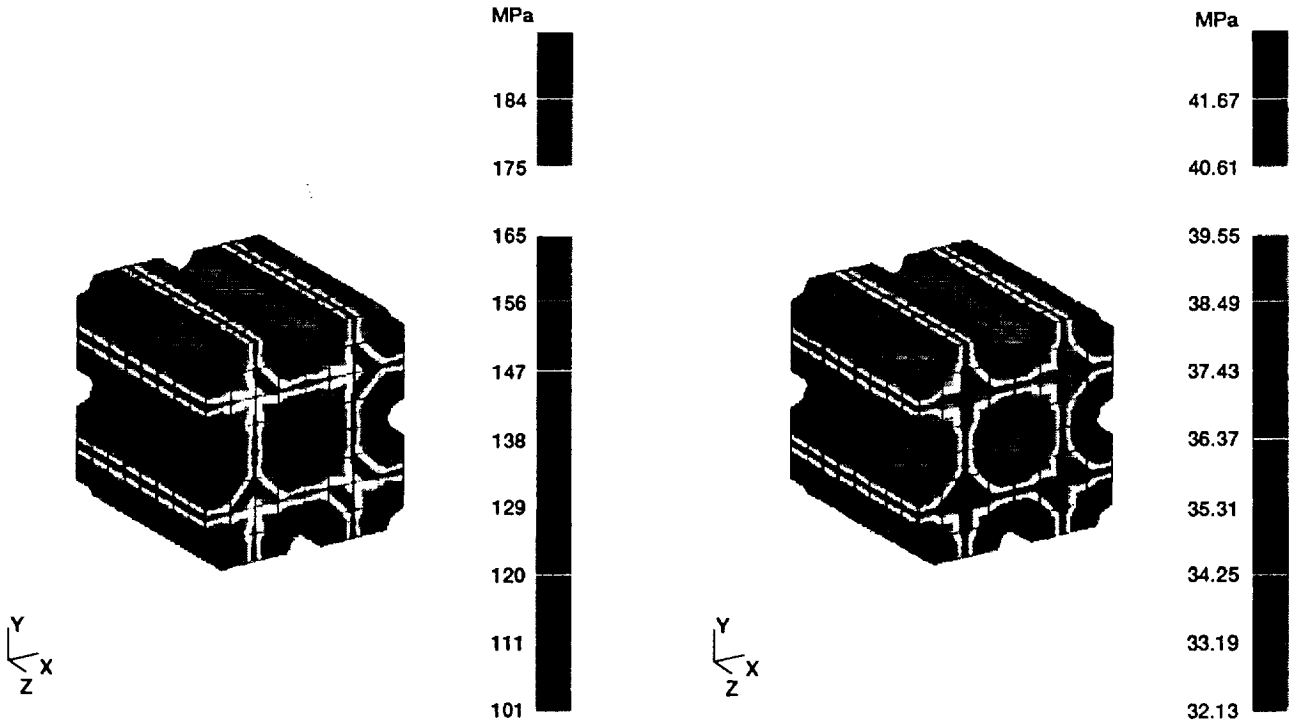

(a) Under cold-worked conditions.

(b) Under annealed material conditions.

Figure 7.—Predicted RT, longitudinal residual stress on the Cu matrix, after cooldown from 542 °C of a 9 v/o W/Cu composite.

PRECEDING PAGE BLANK NOT FILMED

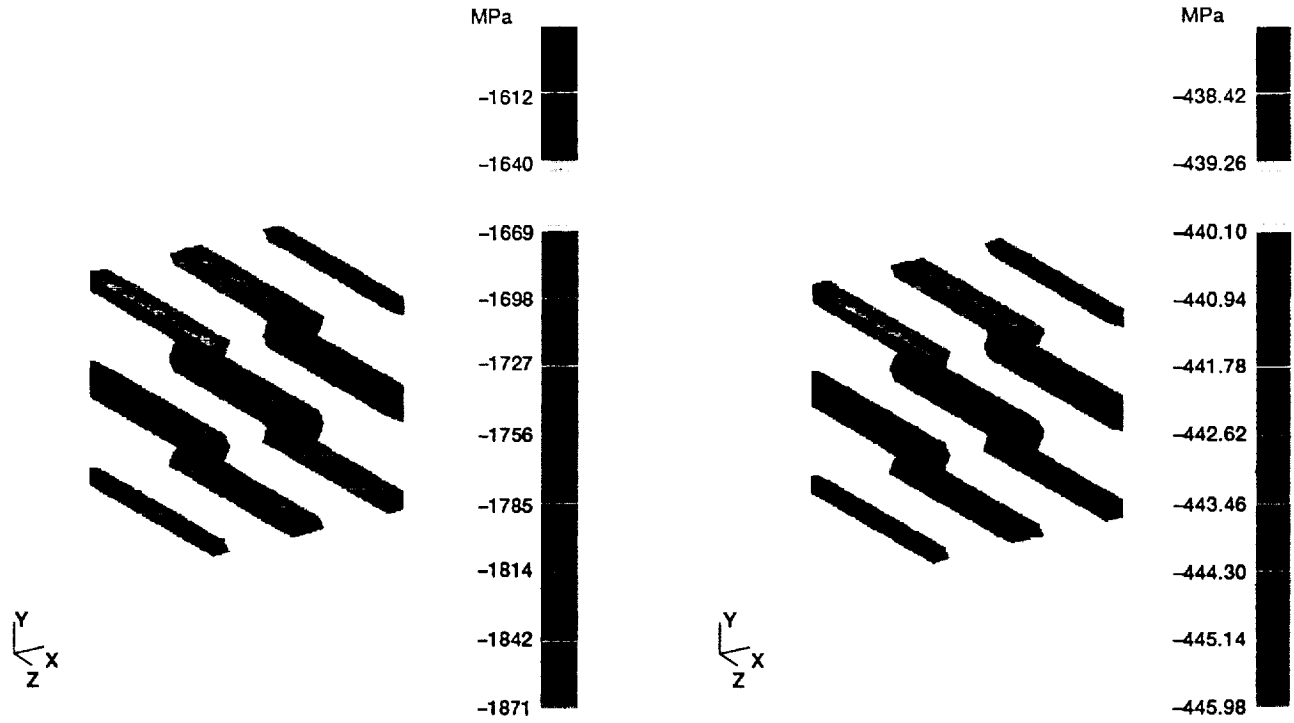

(a) Under cold-worked conditions.

(b) Under annealed material conditions.

Figure 8.—Predicted RT, longitudinal residual stress on the W fibers, after cooldown from 542 °C of a 9 v/o W/Cu composite.

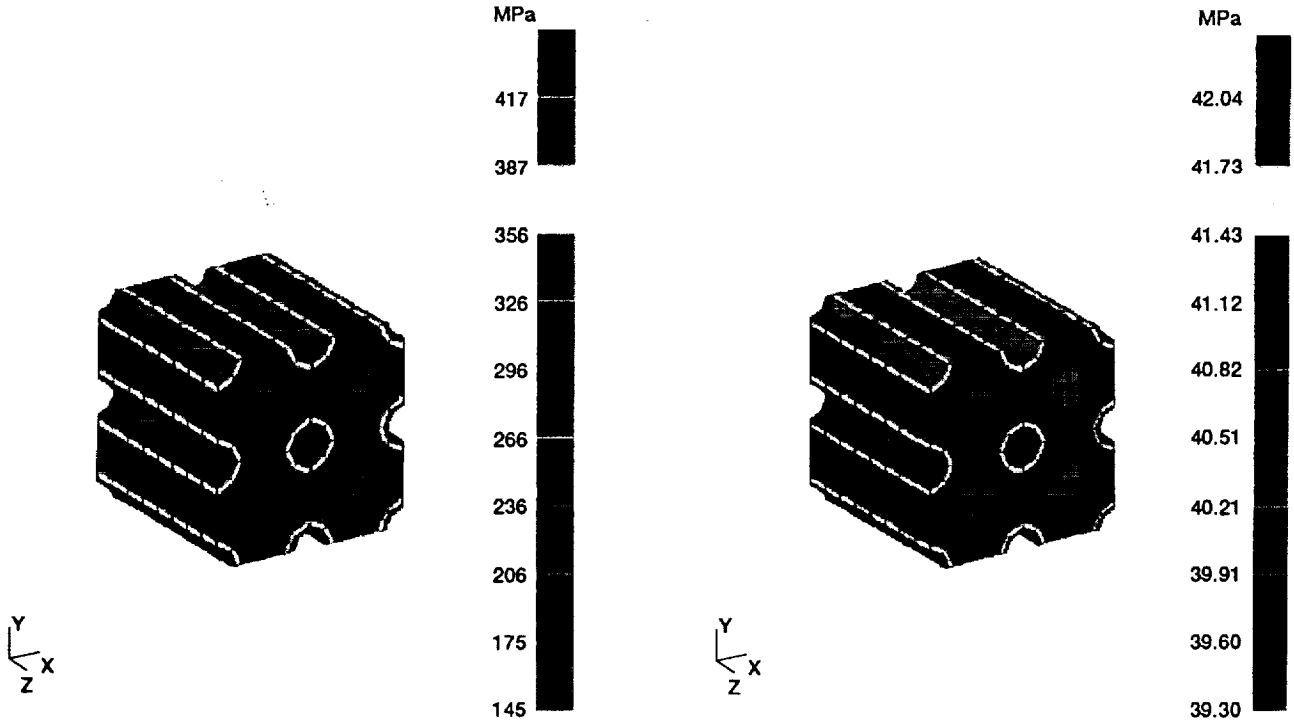

(a) Under cold-worked conditions.

(b) Under annealed material conditions.

Figure 9—Predicted RT, equivalent Mises stress on the Cu matrix, after cooldown from 542 °C of a 9 v/o W/Cu composite.

PRECEDING PAGE BLANK NOT FILMED

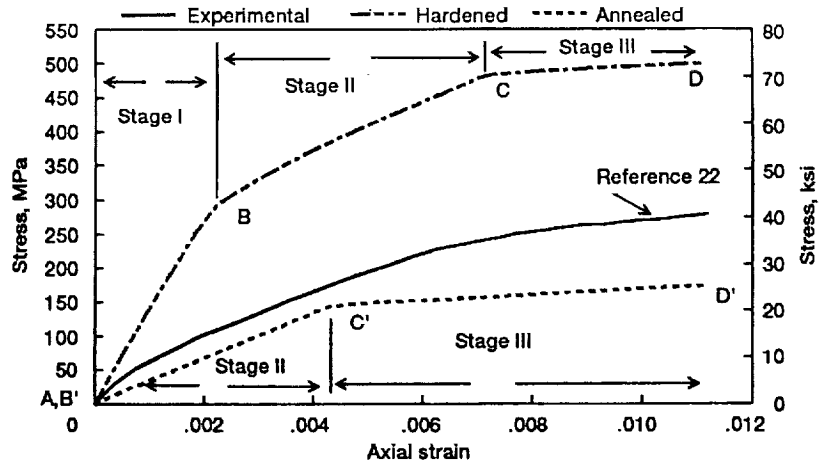

Figure 10.—Predicted and experimental, room temperature, tensile stress-axial strain curves for the unidirectional, 9 v/o W/Cu composite.

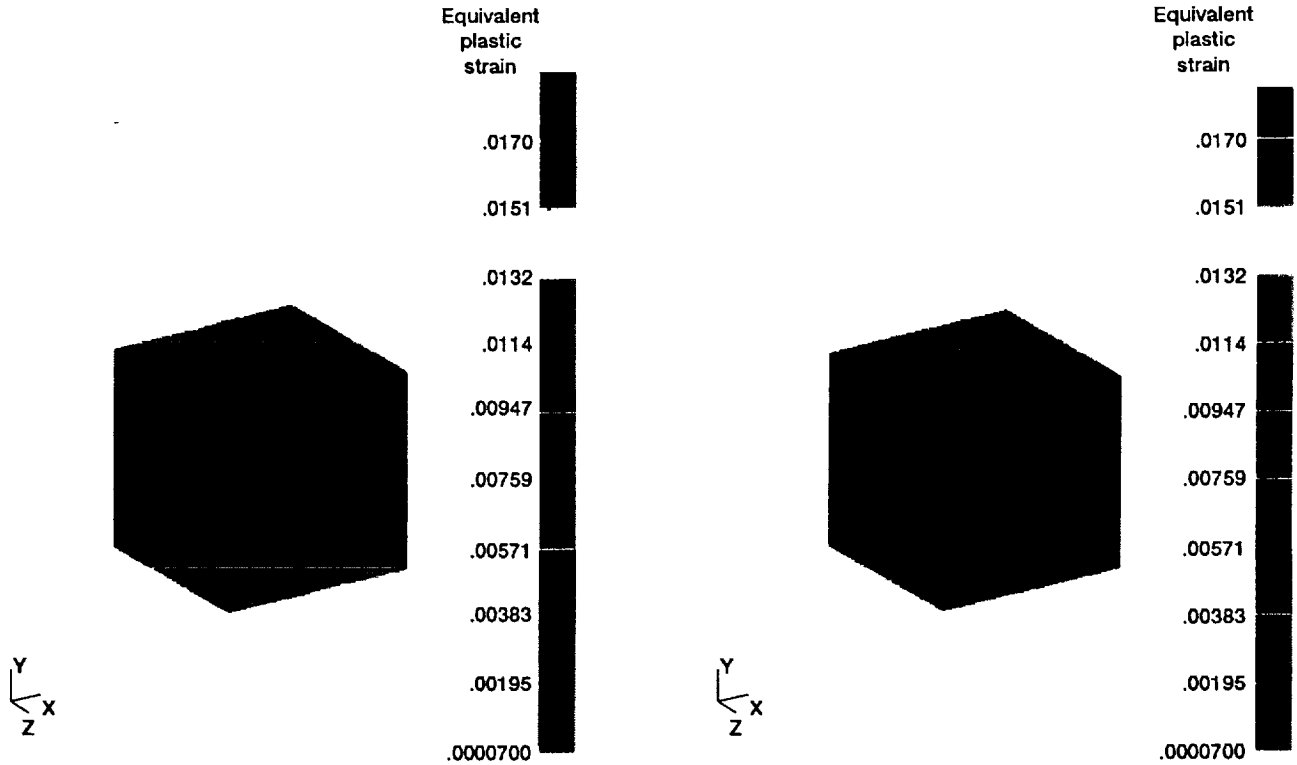

(a) Under cold-worked conditions.

(b) Under annealed material conditions.

Figure 11.—Predicted plastic deformation after loading to 145 MPa.

PRECEDING PAGE BLANK NOT FILMED

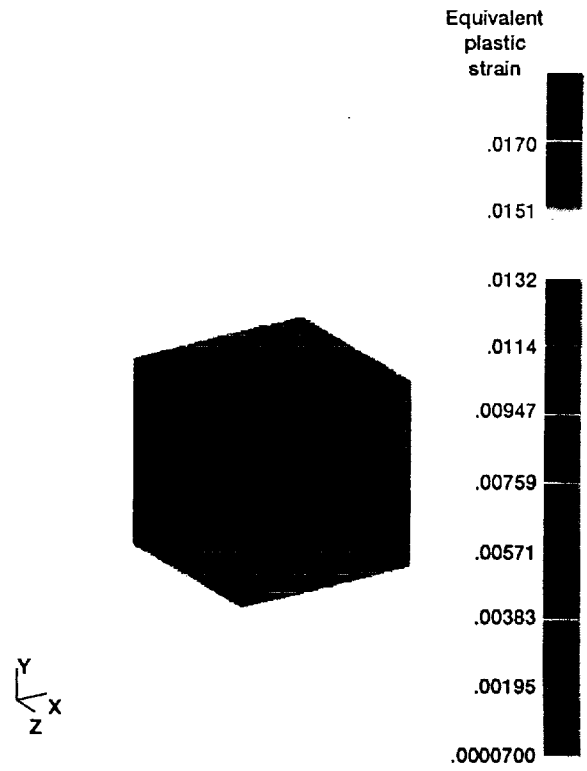

(a) Under cold-worked conditions.

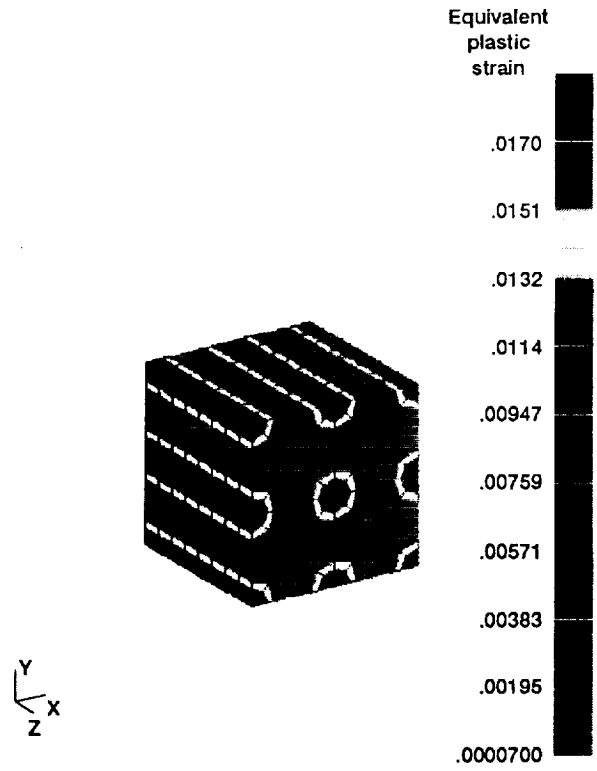

(b) Under annealed material conditions.

Figure 12.—Predicted plastic deformation after loading to 175 MPa.

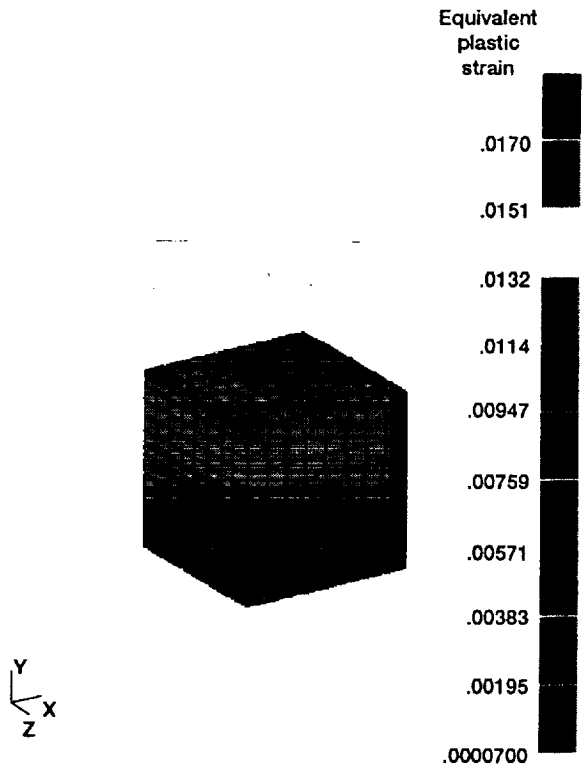

Figure 13.—Predicted plastic deformation after loading to 280 MPa under cold-worked material conditions.

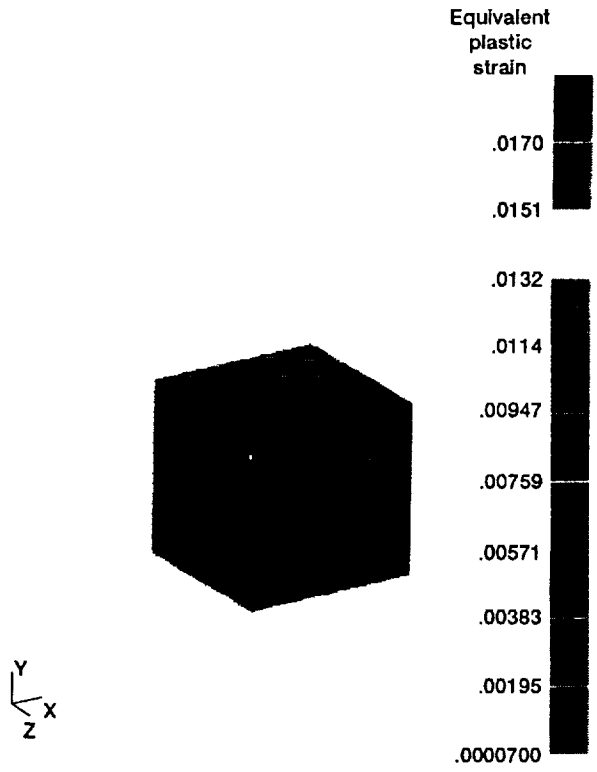

Figure 14.—Predicted plastic deformation after loading to 380 MPa under cold-worked material conditions.

PRECEDING PAGE BLANK NOT FILMED

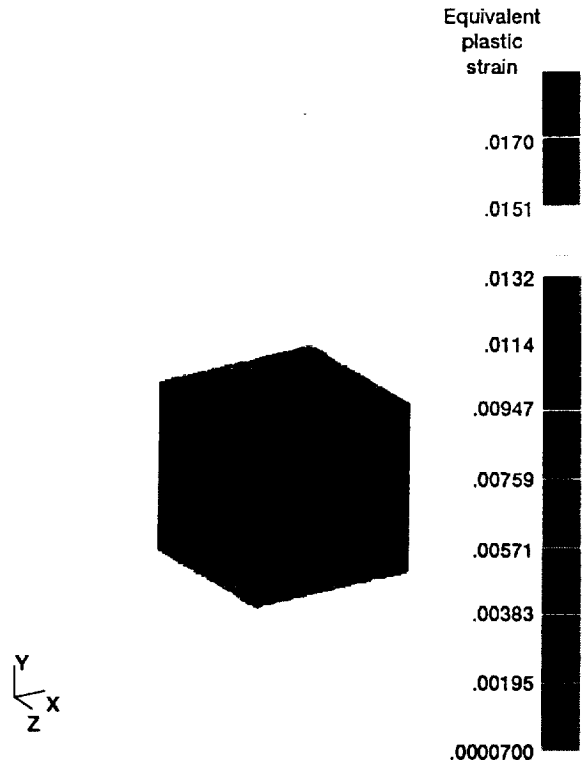

Figure 15.—Predicted plastic deformation after loading to 480 MPa under cold-worked material condtions.

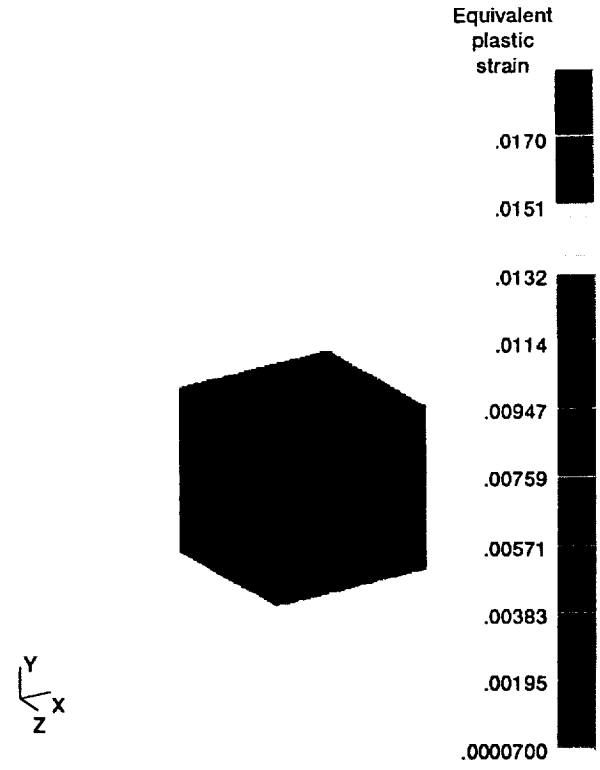

Figure 16.—Predicted plastic deformation after loading to 500 MPa under cold-worked material condtions.

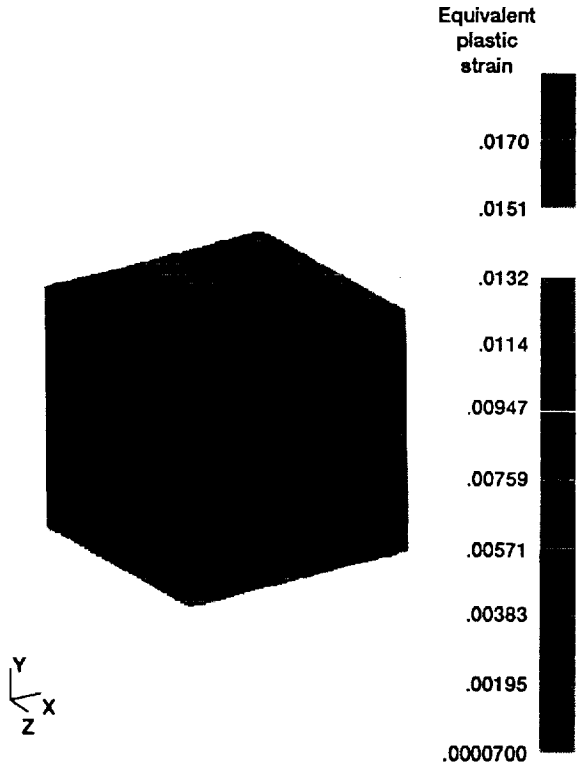

Figure 17.—Predicted plastic deformation after loading to 70 MPa under annealed material conditions.

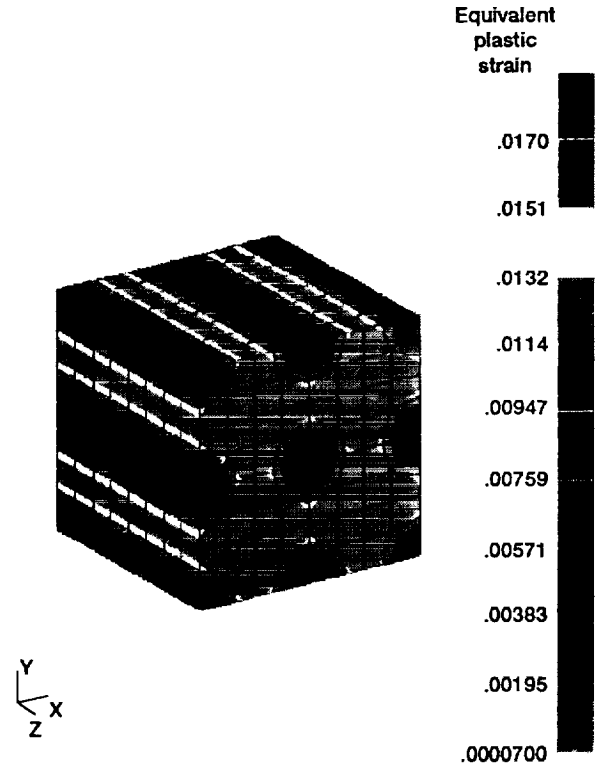

Figure 18.—Predicted plastic deformation after loading to 160 MPa under annealed material conditions.

PRECEDING PAGE BLANK NOT FILMED

REPORT DOCUMENTATION PAGE

Form Approved
OMB No. 0704-0188

Public reporting burden for this collection of information is estimated to average 1 hour per response, including the time for reviewing instructions, searching existing data sources, gathering and maintaining the data needed, and completing and reviewing the collection of information. Send comments regarding this burden estimate or any other aspect of this collection of information, including suggestions for reducing this burden, to Washington Headquarters Services, Directorate for Information Operations and Reports, 1215 Jefferson Davis Highway, Suite 1204, Arlington, VA 22202-4302, and to the Office of Management and Budget, Paperwork Reduction Project (0704-0188), Washington, DC 20503.

1. AGENCY USE ONLY (*Leave blank*)	2. REPORT DATE	3. REPORT TYPE AND DATES COVERED
	September 1993	Technical Memorandum

4. TITLE AND SUBTITLE

Elastic-Plastic Finite Element Analyses of an Unidirectional, 9 vol % Tungsten Fiber Reinforced Copper Matrix Composite

5. FUNDING NUMBERS

WU-510-01-50

6. AUTHOR(S)

Jose G. Sanfeliz

7. PERFORMING ORGANIZATION NAME(S) AND ADDRESS(ES)

National Aeronautics and Space Administration
Lewis Research Center
Cleveland, Ohio 44135-3191

8. PERFORMING ORGANIZATION REPORT NUMBER

E-8045

9. SPONSORING/MONITORING AGENCY NAME(S) AND ADDRESS(ES)

National Aeronautics and Space Administration
Washington, D.C. 20546-0001

10. SPONSORING/MONITORING AGENCY REPORT NUMBER

NASA TM-106304

11. SUPPLEMENTARY NOTES

Responsible person, Jose G. Sanfeliz, (216) 433-3348.

12a. DISTRIBUTION/AVAILABILITY STATEMENT

Unclassified - Unlimited
Subject Category 24

12b. DISTRIBUTION CODE

13. ABSTRACT (*Maximum 200 words*)

Micromechanical modeling via elastic-plastic finite element analyses were performed to investigate the effects that the residual stresses and the degree of matrix work hardening (i.e., cold-worked, annealed) have upon the behavior of a 9 vol %, unidirectional W/Cu composite, undergoing tensile loading. The inclusion of the residual stress-containing state as well as the simulated matrix material conditions proved to be significant since the Cu matrix material exhibited plastic deformation, which affected the subsequent tensile response of the composite system. The stresses generated during cooldown to room temperature from the manufacturing temperature were more of a factor on the annealed-matrix composite, since they induced the softened matrix to plastically flow. This event limited the total load-carrying capacity of this matrix-dominated, ductile-ductile type material system. Plastic deformation of the hardened-matrix composite during the thermal cooldown stage was not considerable, therefore, the composite was able to sustain a higher stress before showing any appreciable matrix plasticity. The predicted room temperature, stress-strain response and deformation stages under both material conditions represented upper and lower bounds characteristic of the composite's tensile behavior. The initial deformation stage for the hardened material condition showed negligible matrix plastic deformation while for the annealed state, its initial deformation stage showed extensive matrix plasticity. Both material conditions exhibited a final deformation stage where the fiber and matrix were straining plastically. The predicted stress-strain results were compared to the experimental, room temperature, tensile stress-strain curve generated from this particular composite system. The analyses indicated that the actual thermal-mechanical state of the composite's Cu matrix, represented by the experimental data, followed the annealed material condition.

14. SUBJECT TERMS

Metal matrix composites; Tungsten; Copper; Tensile deformation; Tensile tests; Finite element method; Thermal residual stress; Elastic-plastic; Plastic yielding; Plastic flow

15. NUMBER OF PAGES

26

16. PRICE CODE

A03

17. SECURITY CLASSIFICATION OF REPORT	18. SECURITY CLASSIFICATION OF THIS PAGE	19. SECURITY CLASSIFICATION OF ABSTRACT	20. LIMITATION OF ABSTRACT
Unclassified	Unclassified	Unclassified	